land

Article

Changes in the Landform and Water Conditions of the Industri-Alized Urban Area as a Result of Mining Activities

Robert Machowski

Faculty of Natural Sciences, Institute of Earth Science, University of Silesia in Katowice, Będzińska 60, 41-200 Sosnowiec, Poland; robert.machowski@us.edu.pl

Abstract: A particularly large accumulation of mining subsidence basins is characteristic for the Silesian Upland in southern Poland. This region is home to one of Europe's largest coal basins. The objective of the study was to assess the subsidence process on the land surface in an industrialized urban area, as well as their impact on changes in the water cycle. Detailed studies were conducted in an area of 51.26 km^2, which covers urban areas—mainly of Świętochłowice and partly Ruda Śląska and Chorzów, as well as Bytom and Zabrze. In the period 1883–1994 land surface depressions were revealed in an area of 38.8 km^2, which constitutes 75.7% of the study area. In total, the endorheic areas spread over 6.9 km^2. Changes in land reliefs have resulted in distinct water-cycle disturbances at local and regional levels. A generalised water-cycle scheme has been developed for the mining subsidence zone. The main directions of changes in water migration within the endorheic subsidence basin have been indicated, accounting for the situation before and after land subsidence. Consequently, this results in an average excess of 1.7 hm^3 of water per year in the water cycle in these areas.

Keywords: subsidence basin; coal mining; water cycle; Silesian Upland; anthropopression

check for updates

Citation: Machowski, R. Changes in the Landform and Water Conditions of the Industri-Alized Urban Area as a Result of Mining Activities. *Land* **2022**, *11*, 1710. https://doi.org/10.3390/land11101710

Academic Editor: Krish Jayachandran

Received: 17 September 2022
Accepted: 30 September 2022
Published: 2 October 2022

1. Introduction

Water in nature is in constant motion. In natural conditions, water circulation is caused primarily by the energy of solar radiation and gravitational forces. The hydrological cycle being a closed system involves the movement of water between different parts of the hydrosphere. The volumes of water that participate in the circulation at different stages of the circulation are variable, both seasonally and annually [1]. Today, human activity plays an important role in modifying the water cycle. These effects are evident both locally, regionally, and at a larger scale [2–4]. Human interference with water relations is particularly evident in areas where mining activities have taken place and are still pursued. Human impact is evident in both water quality and water quantity. Changes in the local water cycle are, among others, an indirect result of land subsidence that occurs over and in close proximity to mined mineral deposits [5]. Land subsidence is an unintended consequence of underground mineral extraction. The literature is abundant with information on the extent and magnitude of mining subsidence [6–9] but reports on changes in the water cycle are very rare [10]. Some information in this respect has been presented for the Bogdanka Coal Mine located in eastern Poland [11].

In the beginning, the environmental effects of underground mineral extraction were identified solely by way of visual assessment. Subsequently, simple tools were used to measure the magnitude and extent of land subsidence. It was only after detailed topographic maps had been developed that it became possible to analyse changes in land elevation caused by mining subsidence. The use of topographic maps in combination with modern computer software (including GIS tools) has become a common methodology for evaluating land surface changes caused by human activity. These methods make it possible to determine the effects of many years of mining activity [5,12–16]. This type of research is being carried out in old European coalfields where mining began as early as the 19th century. Contemporary changes in land surface are commonly evaluated using tools based on remote-sensing techniques. However, in this case, only short-term assessments are possible, usually going back to the 1990s. These limitations are related to the availability of satellite imagery with sufficient resolution. Remote-sensing techniques have been widely used in studying land subsidence, especially in China, but also in the U.S., India or parts of Europe [17,18].

In addition to its impact on water relations, mining land subsidence also causes a number of changes affecting other components of the geographic environment. This includes damage to rock mass and the subsequent escape of water deeper into the ground [19]. Changes in soil cover and vegetation can also be observed [20]. In places where subsidence becomes apparent, this entails changes in land use. In extreme cases, degraded wastelands are created. This is conducive to the intensification of slope processes, such as runoff, soil creep or landslides. Similar changes to land cover are predicted to occur in the Val d'Aran region in Spain [21].

A particularly large accumulation of subsidence basins is characteristic for the Silesian Upland in southern Poland. This region is home to one of Europe's largest coal basins (Figure 1). The emergence of sedimentation basins (endorheic catchments) in drainless basins became the rationale for determining their role in altering the water cycle in areas affected by mining.

2. Materials and Methods

2.1. Study Area

In the Silesian Upland located in southern Poland, there are areas whose natural environment has been largely transformed by human activity (Figure 1). Such a spectacular range of changes in land morphology and water relations is rarely seen on a European or even global scale. Underground mineral extraction played a decisive role in this process. Underground mining has resulted in the formation of extensive subsidence basins and numerous spoil tips generated during the extraction of the deposit and its subsequent processing. In the central part of the Silesian Upland, covering urban areas—mainly of Świętochłowice and partly Ruda Śląska and Chorzów, as well as Bytom and Zabrze—there is an area of 51.26 km^2 where anthropogenic transformation of the environment is a common landscape element (Figure 1).

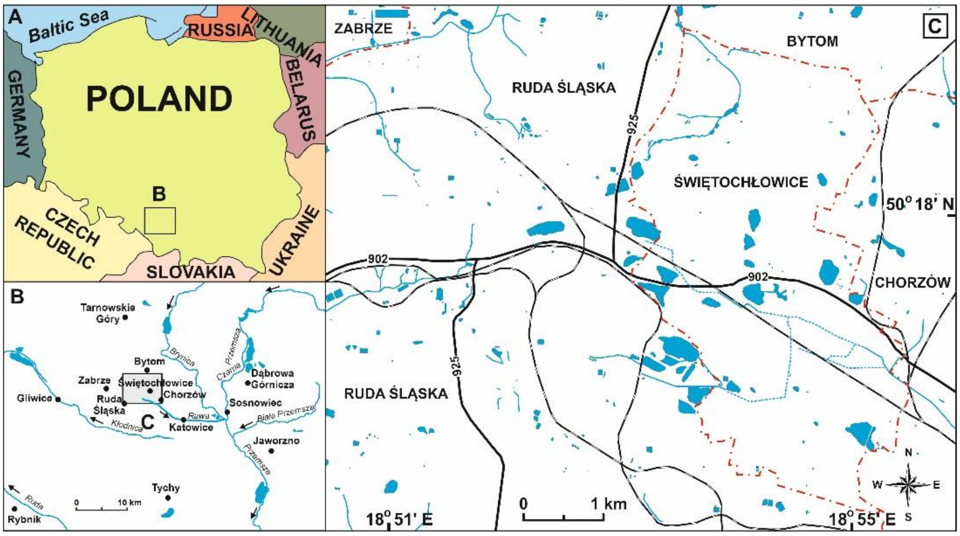

Figure 1. Location of the study area in southern Poland.

Sediments from the Holocene and Pleistocene age are deposited on the land surface within the study area. Much older rocks, classified as Triassic and Carboniferous, are also exposed (Figure 2). Geological formations from the Holocene age are generally represented by sands and gravels that fill the river valleys. The study area is dominated by extensive land covers composed of sands, gravels, and clays that formed during the Pleistocene age. Triassic limestones, dolomites, marls, and claystones are deposited in a small section in the north-eastern part of the area. Throughout the study area, coal-bearing carboniferous rocks appear as scattered pockets, which, under cover of younger sediments, form the geological core of the study area [22].

Thick coal seams are deposited between the layers made up essentially of mudstones, claystones, sandstones and conglomerates. These deposits have been the subject of intensive underground mining activity in the past. Several mining operations were active in the study area. As early as 1853, hard coal started to be produced from deposits located in Świętochłowice. Subsequent mines were started at 10-year intervals: 1863, 1873, 1883. Most of them have been in operation for over 100 years and the last of the mines operating in the area is currently in liquidation. Coal was produced in these mines from 5 to even 19 seams, the thickness of which varied from 0.5 m to 9 m. Underground mining was carried out at depths varying from 40 to 800 m below sea level. In a small section of the northern part of the study area, zinc and lead ores were also extracted [12,22]. Nowadays, the hydrotechnical works conducted in the mine workings include drainage of the rock mass. These operations are conducted to protect coal seams that are being mined in mines located adjacent to the study area from flooding [13].

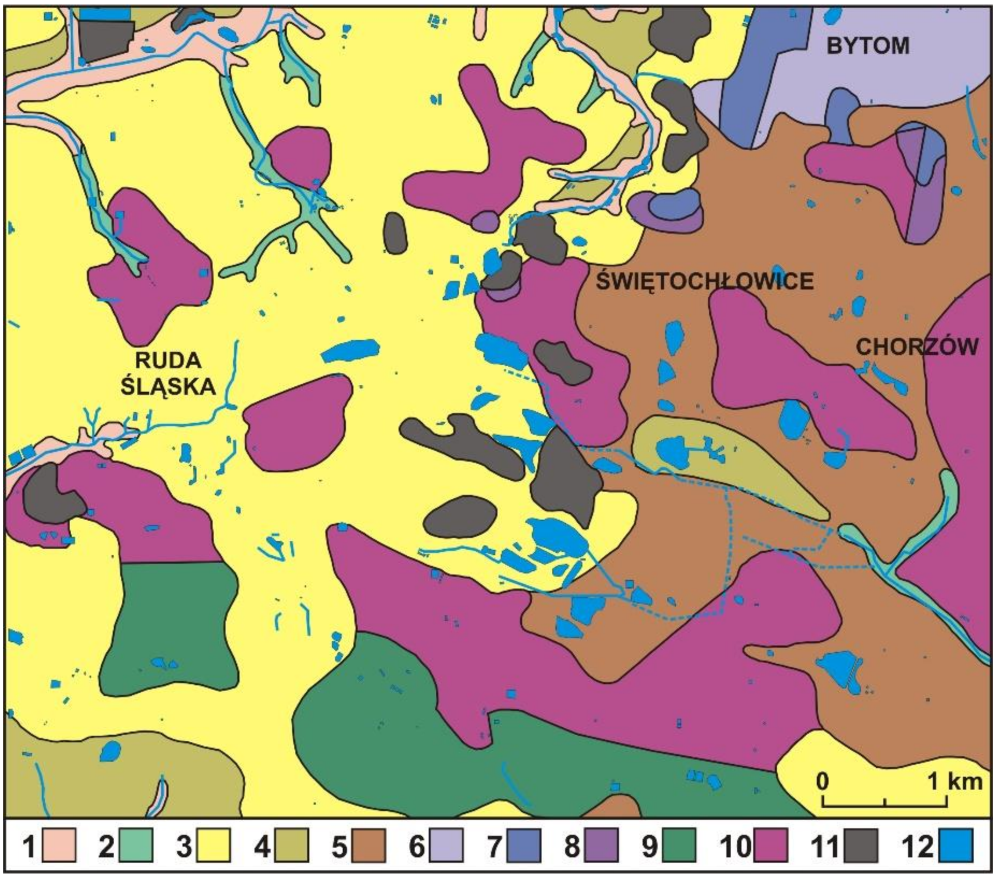

Figure 2. Geological structure exposed on the surface of the study area (after [22] simplified): 1—river sands and gravels of floodplain terraces, 2—river diluvial sands, gravels and silts, 3—residual clays and sands 4—fluvioglacial sands and gravels, 5—tills, 6—limestones, 7—dolomites, marls, limestones and claystones, 8—sands, sandstones, clays, claystones and mudstones, 9—mudstones and claystones with interbeddings of sandstones and tuffites as well as hard coal—mudstone series, 10—sandstones and conglomerates with interbeddings of clays and mudstones as well as hard coal—Upper Silesian sandstone series, 11—spoil tips and embankments, 12—watercourses and reservoirs.

2.2. Research Methods

Land relief changes were determined from cartographic materials. As part of the geomorphological mapping according to the guidelines proposed by the [23] distinctive land relief features (e.g., subsidence basins, spoil tips) were identified and mapped. The study made use of Prussian topographic maps (Messtischblätter) made at the end of the 19th century at a scale of 1:25,000 [24,25] and Polish topographic maps at a scale of 1:10,000 from the last decade of the 20th century [26]. To make both maps comparable, the 19th century maps were calibrated to the current system of coordinates. This was done by overlaying the current layout on the Messtischblätter maps. This allows for a comparative spatial analysis of the state of the environment as depicted on the archival map with the current situation. An excellent resource for this purpose is provided by GIS tools that allow fitting maps based on specific topographic landmarks such as churches, road junctions, etc. Geographic coordinates read from contemporary maps are determined for such structures. The Messtischblätter maps were then fitted based on a first-order affine transformation. Multiple landmarks located in the study area were used for this purpose. Calibration was performed using the ArcMap 10 software. To capture the extent of change in land surface relief, two digital terrain models were prepared for the years 1883 and 1994. The models were produced in the Map Info Professional 10.0 software using the Vertical Mapper tool. The models were used to obtain data on changes in relative and absolute elevation as well as gradients. These studies were complemented by an identification of the geological structure of the study area.

Changes in the water cycle in the zone of mining subsidence within the area were determined on the basis of field, laboratory and desktop studies. Detailed hydrological mapping was performed as part of the field study, consisting of identifying objects related to surface waters [27].

Quantitative changes in the water cycle were determined from collected hydro-meteorological data. Total monthly precipitation values from 1961 to 2020 were used in the calculations. Precipitation was measured at the "Lipiny" precipitation measurement station located in the central part of the study area. The data are from the website of the Institute of Meteorology and Water Management—National Research Institute. Precipitation numbers for each of the subsidence basins were calculated as average annual precipitation from 1961–2020, which was then multiplied by the surface area of each of the endorheic catchments. The calculation uses the following formula [28]:

$$V\ [m^3] = P\ [m] * A\ [m^2] \tag{1}$$

where V is average annual precipitation volume, P is average annual precipitation and A is area of individual endorheic catchments.

Evapotranspiration is a complex process and one of the most difficult water balance items to estimate. Multiple approaches have been used to assess evapotranspiration, from direct field surveys to a variety of mathematical formulas that take into account one or more meteorological factors [29–31]. To this end, experimental models have been developed to estimate evapotranspiration using limited data. Models based exclusively on temperature are the most commonly used methods for estimating evapotranspiration, as direct measurement of evaporation over such a diverse area is virtually impossible [32–34]. The inability to conduct evaporation measurements for different areas within the catchment studied and the amount of meteorological data available resulted in the decision to use in the calculations the formula developed by Kuzin. In Poland, this is a frequently used method for calculating field evaporation [13,28,35,36]. This method is used to calculate evapotranspiration under official government programmes aimed at preventing water shortages in Poland [37].

The amount of evaporation from the water bodies that are located within endorheic subsidence basins was also included in the calculations. Ivanov's formula [38], which relates the amount of evaporation from the water surface to the average monthly temperature and average monthly relative humidity of atmospheric air, was used in the calculations:

$$E = 0{,}0018(25 + t)^2 * (100 - f) \quad (2)$$

where E—total monthly evaporation water [mm], t—average monthly air temperature [°C], f—average monthly relative atmospheric air humidity [%].

Calculations performed for the 1961–2020 multiyear period were used in determining the amount of average annual evaporation. Measurement data were also obtained from the website of the Institute of Meteorology and Water Management—National Research Institute. A formula was used to calculate the amount of evaporation from endorheic areas [28]:

$$E\ [m^3] = H\ [m] * A\ [m^2] \quad (3)$$

where E is average annual evaporation volume, H is average annual evaporation as the sum of evapotranspiration and free-surface evaporation from water bodies and A is area of individual endorheic catchments.

Directly in the field, the factors that affect changes in the water cycle in the study area were identified and then analysed.

3. Results

In the late 19th century, the process of consolidating individual small mining fields into larger mines began in the study area. During this time, the impact of underground mining on land reliefs and water relations was relatively minor. The landscape was already semi-urbanized and industrial in nature. The areas with the lowest absolute elevation values (238 m above sea level (a.s.l.)) were characteristic of the river valley bottom, which is located in the north-western sector of the study area (Figure 3). The maximum elevation of 315 m a.s.l. was reached by elevated areas located in the southwestern part of the study area. Elevation differences at that time reached the value of 77 m. The dominant areas were located at elevations between 280.1–300.0 m a.s.l., which accounted for nearly 58% of the described area. Slightly more than 20% included areas with elevations between 300.1 m and 320.0 m a.s.l. The smallest share of just over 3% included areas with the lowest elevations (Table 1). The land relief was dominated by sloped areas with a low gradient (1.1°–3.0°), which accounted for 36.6% of the study area. Areas with slightly larger gradients up to 5° covered another 25.5%. The smallest proportion was the land with the steepest gradients, above 9°, which amounted to 7.3% (Table 2). By the end of the 19th century, the total length of the river network in the study area was 37.47 km. There were 192 anthropogenic reservoirs with a total surface area of 31.4 ha. The average reservoir surface area was less than 0.18 ha.

Table 1. Changes in absolute elevations of the study area from 1883 to 1994.

Elevation [m a.s.l.]	1883		1994		1883–1994
	[km^2]	[%]	[km^2]	[%]	Δ%
240.0–260.0	1.59	3.1	3.23	6.3	3.2
260.1–280.0	9.53	18.6	14.86	29.0	10.4
280.1–300.0	29.63	57.8	25.94	50.6	−7.2
300.1–320.0	10.51	20.5	7.13	13.9	−6.6
320.1–340.0	0.00	0.0	0.10	0.2	0.2
∑	51.26	100.0	51.26	100.0	0.0

Table 2. Land gradients in the study area from 1883 to 1994.

Gradient [°]	1883		1994		1883–1994
	[km^2]	[%]	[km^2]	[%]	Δ%
0.0°–1.0°	6.05	11.8	11.89	23.2	11.4
1.1°–3.0°	18.76	36.6	21.99	42.9	6.3
3.1°–5.0°	13.07	25.5	9.02	17.6	−7.9
5.1°–9.0°	9.64	18.8	4.72	9.2	−9.6
9.1°–20.0°	3.43	6.7	2.72	5.3	−1.4
>20.0°	0.31	0.6	0.92	1.8	1.2
∑	51.26	100.0	51.26	100.0	0.0

By the end of the 20th century, the study area had been developed into a traditional industrial landscape and, locally, had taken on a post-industrial character. The growth of the areas with the lowest elevations was clearly visible during this time. In the range of 240.0–260.0 m a.s.l., the actual surface area increased from 1.59 km^2 at the end of the 19th century to 3.23 km^2 (6.3%) at the end of the 20th century. At elevations between 260.1 and 280.0 m a.s.l., there was an increase of just over 10% from 9.53 km^2 to 14.86 km^2. There has been a marked decrease in the proportion of land above 280 m a.s.l. In 1994, the actual area of this land decreased by a total of 7.07 km^2. At that time, areas of anthropogenic genesis located at elevations above 320 m a.s.l. were identified that did not occur under natural conditions (Table 1). These were artificially created slag tips for waste generated in metal smelting processes. They were located in the central part of the surveyed area, within the boundaries of the Huta Pokój steelworks. The culminations of these elevations reached 322 m a.s.l. The lowest-lying areas (232 m a.s.l.) included the southern part of the aforementioned river valley in the north-western part of the study area, within which an elongated subsidence basin was formed (Table 3, Figure 4).

After 111 years, the elevation differences within the area increased to 90 m. The patterns described above influenced similar changes observed in the gradients. By the end of the 20th century, there was a 17.7% increase in the areas with the lowest gradients (to 3°). Thus, there was an apparent 18.9% decrease in the proportion of areas with gradients up to 20°. In terms of areas with the steepest gradients, above 20°, a 1.2% increase was observed (Table 2).

Changes in the relief caused by underground mining operations, which has lasted for over 100 years in the study area, have directly affected the transformation of water relations. This is especially true for mining subsidence zones. The subsidence of the area as a result of deep mining of hard coal and, in the northern part, zinc and lead ores, covered a surface area of 38.8 km^2, a proportion as high as 75.7% of the study area. The most frequent subsidence was up to 10 m (61.8%). However, in some places the maximum subsidence reached nearly 30 m (Table 3, Figure 4). The areas with the greatest risk of subsidence are those where underground mining was carried out in the past at shallow depths (to 100 m below the ground). This type of mining involved sites scattered throughout the study area. Many years of mining and smelting activities in the area have simultaneously contributed to the increase in absolute elevations. The higher-lying areas covered a total surface area of 6.46 square kilometers, representing a share of 12.6% (Table 3, Figure 4). Small changes within ±1 m affected 6 km^2 (11.7%).

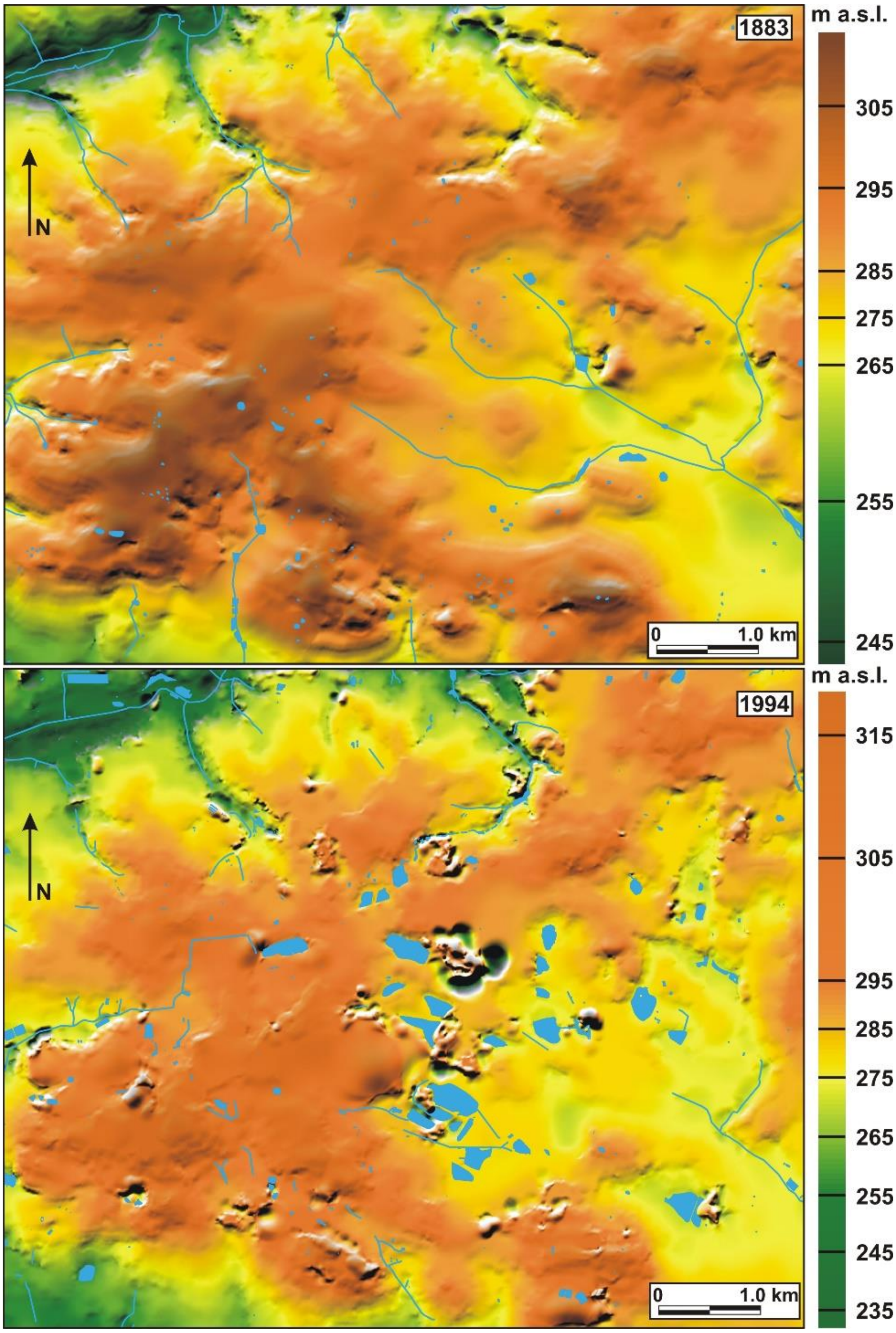

Figure 3. Land relief and surface water network in 1883 and 1994.

Table 3. Anthropogenic changes in relative elevations in the study area from 1883 to 1994.

Changes in Elevation	[km^2]	[%]
20.1 m–30.0 m	0.21	0.4
10.1 m–20.0 m	0.77	1.5
5.1 m–10.0 m	1.38	2.7
1.1 m–5.0 m	4.10	8.0
−1.0 m–1.0 m	6.00	11.7
−1.1 m–−5.0 m	14.46	28.2
−5.1 m–−10.0 m	17.22	33.6
−10.1 m–−20.0 m	6.61	12.9
−20.1 m–−30.0 m	0.51	1.0

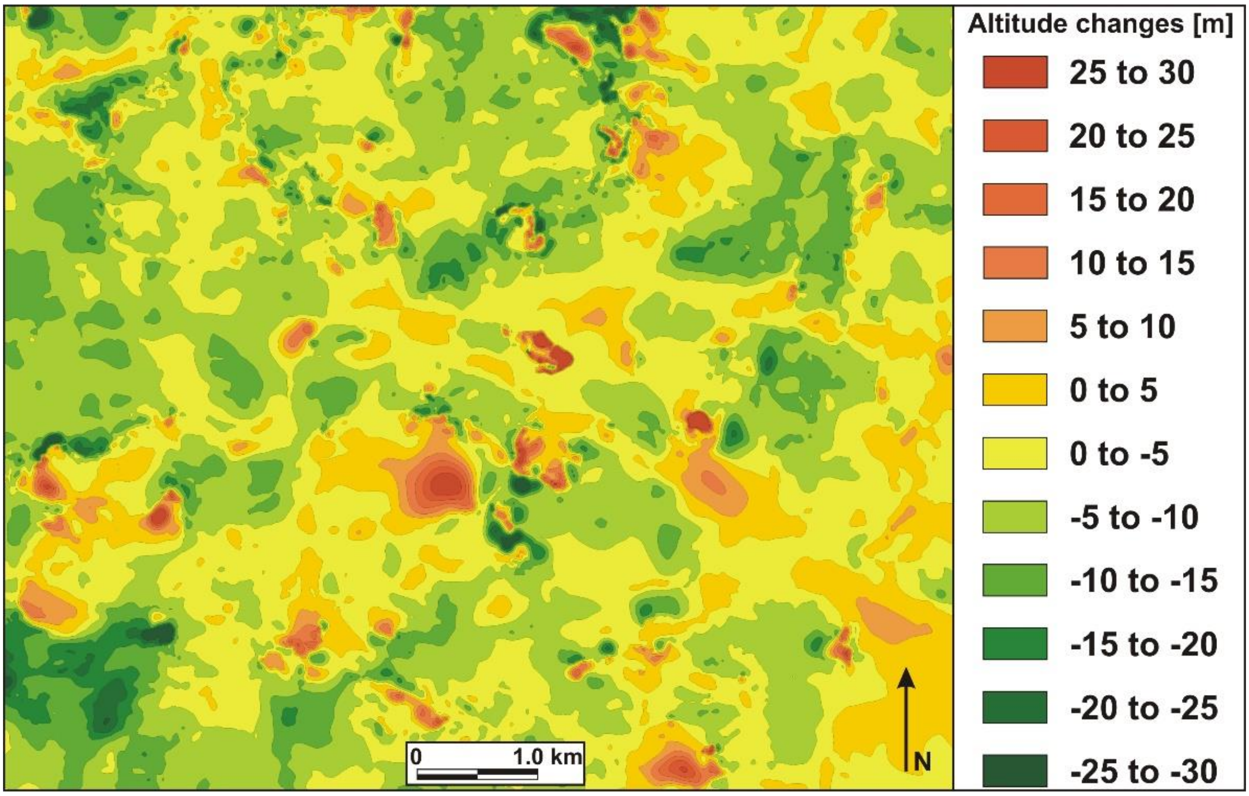

Figure 4. Spatial distribution of anthropogenic changes in elevations from 1883 to 1994.

By the end of the 20th century, the total length of the river network in the described area had decreased by 8.31 km, to 29.16 km. There were 322 anthropogenic water bodies functioning in the geographic environment during this period—an increase by 130 artificial lakes. Limnic waters covered a total surface area of 129.4 ha. The average reservoir surface area was 0.40 ha. The study area is dominated by small and very small water bodies. The largest include artificial lakes such as: "Edward"—9.69 ha, "Marcin"—6.4 ha and "Kokotek"—5.31 ha (Figure 5).

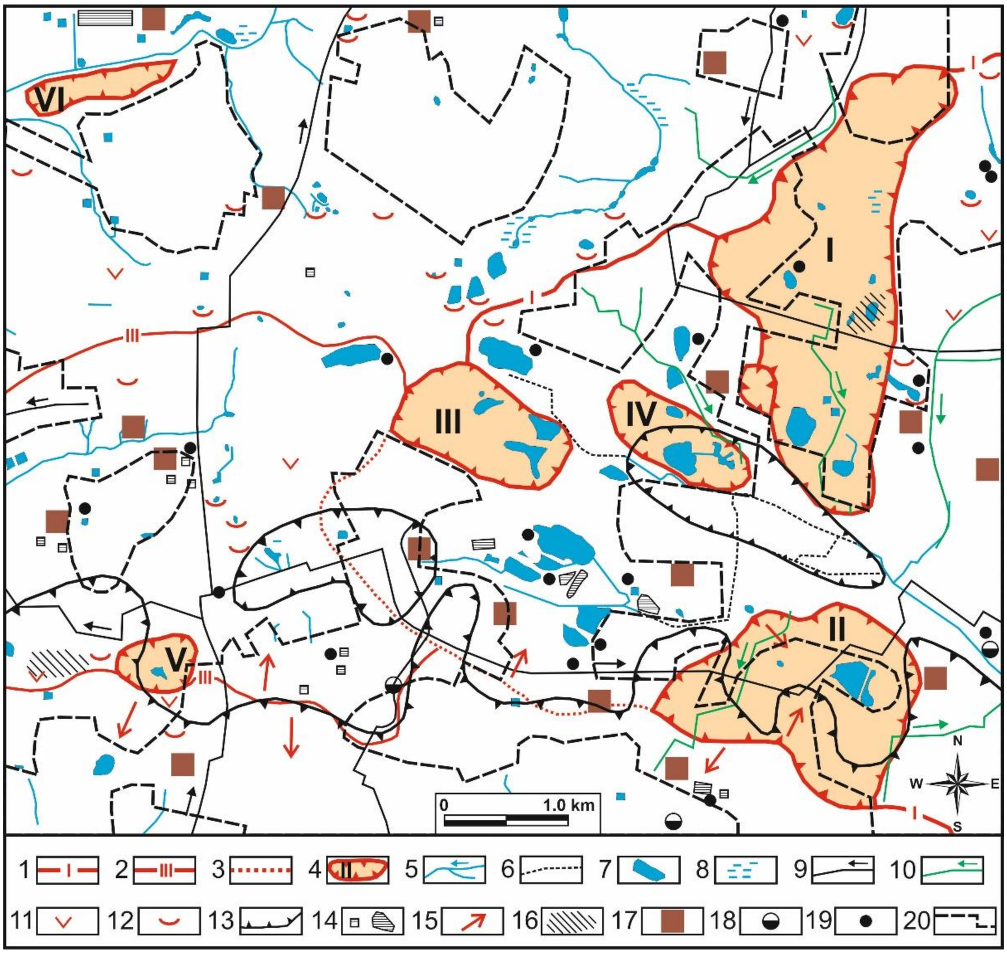

Figure 5. Water relations of the study area in the late 20th and early 21st centuries (after [39] modified and simplified): 1—watershed of the 1st. order, 2—watershed of the 3rd. order, 3—uncertain watershed, 4—watershed of closed drainage basin of the evapotranspiration type, 5—water courses, 6—water courses covered, 7—water reservoirs, 8—wetlands and intermittent wetlands, 9—transfers of water polluted by industrial wastewater, 10—transfers of clean water, 11—closed drainage basin hollows of the absorbing (infiltration) type, 12—closed drainage basin hollows of the evapotranspiration type, 13—extend of intensive anthropogenic landform change, 14—sedimentation tank, 15—directions of surface flow and local shallow undergrounds flows, 16—areas waterlogged by water flows diverted due to economic activities, 17—sewage treatment plant, 18—water treatment plant, 19—pumping-station, 20—sewage coverage.

The observed changes in water relations that affect surface waters in particular are also expressed in the form of quantitative changes in the water cycle. In the period prior to underground mineral extraction, a distinct first-order watershed ran through the study area, delineating the boundaries of two adjacent river drainage basins. In such conditions, the eastern part was drained through the Rawa River to the Brynica, which flows into the Black Przemsza River. The river then joins the White Przemsza and as the Przemsza River it is a tributary of the Vistula, which later flows into the Baltic Sea. The northern part of the area is drained by the Bytomka River and its tributaries. The river flows west, where it joins the Kłodnica River. From the western part of the study area the water flows through the Czarniawka River, which also flows into the Kłodnica River. The outflow from the southern part of the river flowed through small streams feeding the Kochłówka River, also a tributary of the Kłodnica River. The Kłodnica River is a tributary of the Oder, which flows into the Baltic Sea. Changes in land reliefs related with mining activities have locally altered the course of the first order watershed. Nowadays, its course is uncertain along a considerable length, and in some places—practically impossible to delineate. In addition, six drainless depressions were identified in the study area as a result of mining subsidence (Figure 5).

In the Rawa basin there are four basins, the largest in terms of area, and two smaller ones—one in the Bytomka basin and one in the Czarniawka basin. In total, the endorheic areas spread over 6.9 km^2 (Table 4). No such formations were found in areas draining to the Kochłówka River. The formation of these depressions caused visible disturbances in the course of natural processes related to water circulation, which are expressed, among others, in quantitative changes of the water balance for particular drainage basins. The resulting basins are endorheic evapotranspiration sites. They have been "taken out" from the water cycle of the catchment areas within which they previously functioned (Figure 5).

Table 4. Water balance of endorheic basins from subsidence.

Endorheic Area	Area [m^2]		Average Annual Precipitation [m^3]	Average Annual Evaporation [m^3]		Difference [m^3]
	Subsidence Basin	Water Reservoirs		Subsidence Basin	Water Reservoirs	
I	3 107 500	10 000	2 280 451	1 496 744	6 083	777 624
II	2 035 750	6 750	1 494 089	980 530	4 106	509 453
III	803 750	8 750	594 344	387 130	5 323	201 891
IV	527 500	7 500	391 353	254 073	4 562	132 718
V	199 000	1 000	146 300	95 849	608	49 843
VI	192 500	0	140 814	92 719	0	48 095
Σ	6 866 000	34 000	5 047 351	3 307 045	20 682	1 719 624
	6 900 000			3 327 727		

Considering the average annual precipitation from 1961 to 2020 of 731.5 mm in the water balance equation, it was calculated that an average of 140,814 m^3 to 2,280,451 m^3 of water entered each endorheic area per year as a result of precipitation. Average annual precipitation values slightly exceed 5 hm^3 (Table 4). In the study area during the period 1961–2020, the average annual field evaporation amounted to 481.7 mm, which translates into a loss of water from endorheic areas ranging from 92,719 m^3 to 1,502,827 m^3. In total, this results in a loss of 3.3 hm^3 of water per year (Table 4). The calculations allow the conclusion that the excess of water in amount of 48 095 m^3 in basin no. 6 to 777,624 m^3 in basin no. 1 contributes to the first aquifer only to a small extent, due to the poor permeability of the substrate. Rainwater feeds numerous artificial reservoirs. Under natural conditions (prior to mining operations), rainwater from endorheic catchments would feed the surface river network. The greatest losses in this regard are in the Rawa catchment, where total precipitation in the area of the four basins averages 4.76 hm^3 per year. In the Bytomka and Czarniawka catchments these losses are estimated at 0.14 hm^3. From the wetlands, some of the water is directed through a pumping system into the sewer system and then discharged into the river network.

Mining land subsidence initiates the formation of endorheic depressions. In the areas in question, rock mass dewatering continues to protect mines from flooding. Their specific geological structure is reflected by the presence of layers of impermeable sediments at shallow depths in the subsiding rock mass. These types of rock formations effectively retain the water infiltrating into the ground from precipitation. The flow of groundwater is limited to the zone of the basin formed and is local in nature. The emerging subsidence basin forces the water to flow towards its lowest part, which results in the elevation of the water table relative to ground surface (Figure 6). In the five endorheic depressions studied, water appears on the land surface, forming anthropogenic water bodies. These waters do not flow to adjacent areas, and thus the depressions formed are subject exclusively to evapotranspiration. In some areas, excess water is pumped out to the municipal sewage system.

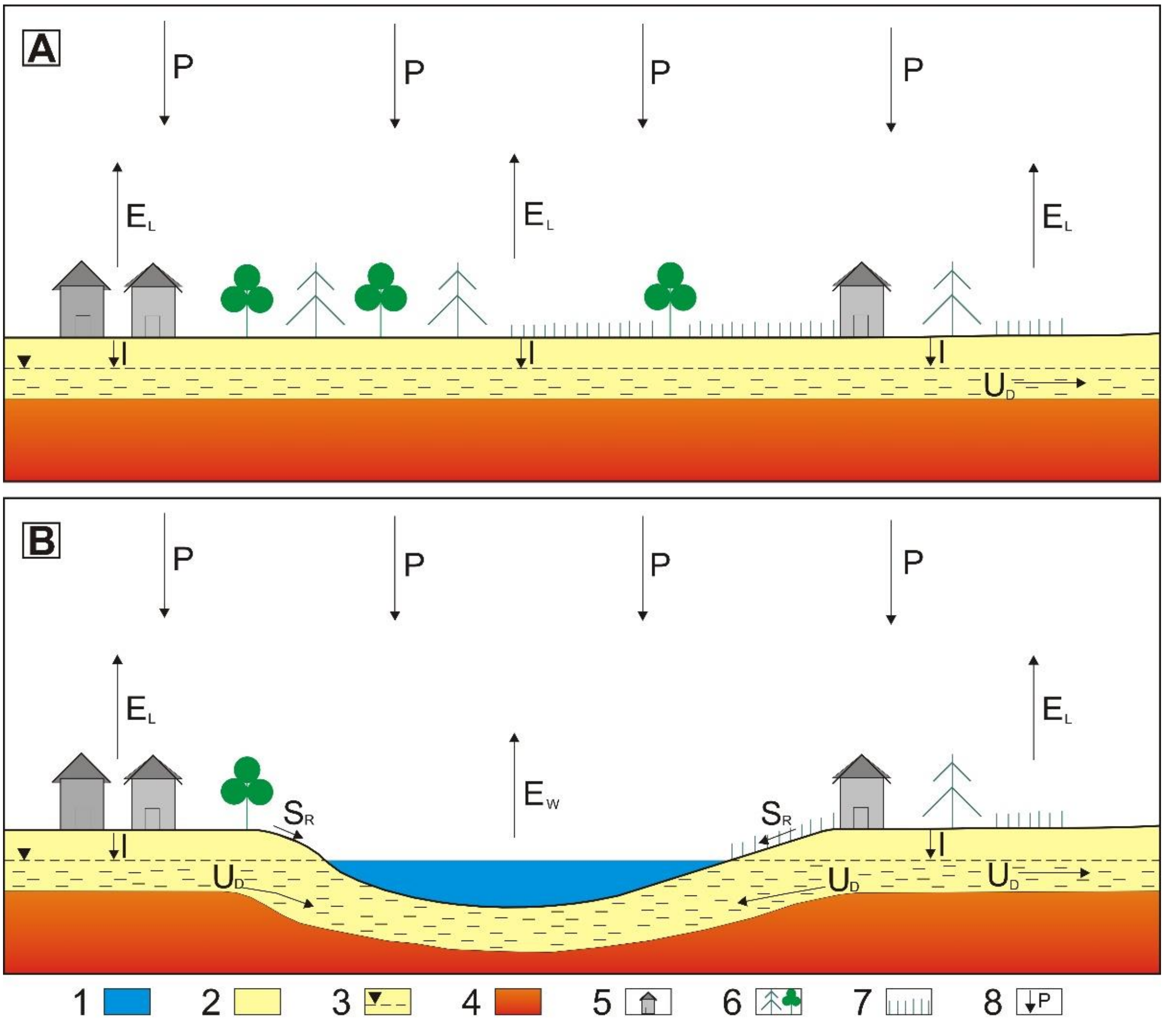

Figure 6. The schematic water cycle in these areas before (**A**) and after (**B**) the emergence of land subsidence: 1—water reservoir, 2—permeable rocks, 3—groundwater level, 4—impermeable sediments, 5—dense and scattered housing, 6—forest and planting, 7—humid and dry meadows, 8—elements of water exchange P—atmospheric precipitations, E_L—evapotranspiration, E_W—free-surface evaporation from water bodies, U_D—groundwater flow, S_R—surface runoff.

4. Discussion

Many years of underground exploitation of mineral resources in the Silesian Upland caused multidirectional changes in the natural geographical environment [40–44]. The negative effects associated with deep underground mining are commonly associated with the appearance of subsidence basins on the land surface, which should be considered as so-called mining damage. It is estimated that land surface depressions as unintended consequences of deep mining of mineral deposits will occur in approx. 1500 km^2 of these areas [45]. Observed hypsometric changes directly affect changes in water relations. Endorheic depressions that modify the water cycle play an important role in this regard. There is usually an increase in surface water resources. A characteristic feature of precipitation is its high seasonal variability (Figure 7). In the past, precipitation most often clearly exceeded water losses associated with field evaporation. Since 2010, the study area has increasingly experienced years when water from precipitation is used entirely for evaporation (Figure 7).

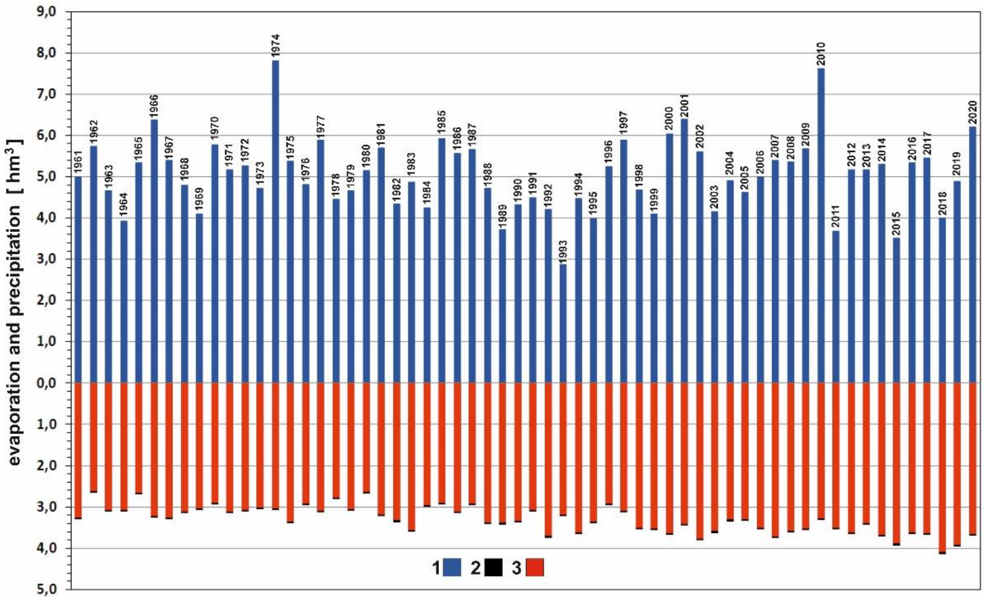

Figure 7. Elements of vertical water exchange in the endorheic basins in the study area from 1961 to 2020: 1—precipitation, 2—free-surface evaporation from water bodies, 3—evaporation.

Changes in the volumes of water involved in the water cycle at its various stages are often cited as an example of the manifestations of global warming [46–48]. These changes are particularly acute in arid and semi-arid climate zones, where a rapid shrinkage of surface water resources is observed [49,50].

When determining changes in the water balance, estimating the amount of evapotranspiration proves to be a difficult issue [51–53]. There are examples of studies in which none of the methods used gave good results [54]. This is especially true for many arid and semi-arid regions where evapotranspiration accounts for significant water loss [55]. A similar situation obtains for the isolated evapotranspiration basins studied. Within these basins, water circulation basically involves two components: precipitation and evaporation. Due to the morphology of the basin and the presence of impermeable sediments in its substrate, there is no groundwater flow between the mining subsidence zone and the adjacent areas (Figure 6). Shallow groundwaters are recharged only by precipitation in the basin zone. The main purpose of the study was to demonstrate some general relationships and patterns related to the impact of mining subsidence basins on local changes in the hydrological cycle.

Endorheic basins created by deep underground extraction of minerals are extremely rarely studied in terms of changes to the water cycle. Much more frequently, such depressions are considered in terms of the course of the geomorphological processes. Research in this field has been conducted in Poland, in the Silesian Upland, as well as in many regions of the world where underground mining of mineral resources takes place [56–58]. Remote sensing related to identifying the extent, magnitude and rate of rock mass subsidence are a very popular research field [17,18,59–62].

The few works that have highlighted the role of anthropogenic depressions in relation to environmental water circulation include reports from China. The impact of land subsidence on changes in water relations was evaluated using the example of seven subsidence basins formed in the Huainan mining area in China. Modelling studies for this area have shown that surface water resources can amount to approximately 905 hm^3 per year in the mining subsidence zone. Only three of these basins are closed areas, whereas the others were created in river valleys and are flow-through [10]. For the same area, a rather interesting study was conducted regarding the possibility of using the basins created by subsidence to intercept flood waves occurring on rivers [63].

In the northern part of the Silesian Upland, a pilot study was conducted in 2018 within one of the most extensive subsidence basins. This study found that on average, 3.1 hm^3 of excess water occurs each year from precipitation [28].

Wetlands and bodies of water that have been created by unplanned mining subsidence quite often become research sites. Many such water reservoirs have been identified in the Silesian Upland, where even the so-called Upper Silesian Anthropogenic Lake District has been distinguished [64]. It is much less common to find information from other regions of the world. The formation of a few wetlands and water reservoirs of such origin has been confirmed, among others, in the area of the Czech Republic [15], Germany [16] or China [65–67].

The results obtained in this study are also of a broader nature and have applications. The results of the study can be used in developing predictions of land subsidence and changes in the water cycle in connection with nurturing biodiversity, and remodelling plant species composition and animal habitats [68]. Where mining subsidence emerges, this results in the modification of the local water cycle, which should be taken into account in the small retention programmes developed. Subsidence and water-cycle data should be taken into account when designing or modifying rainwater and snowmelt drainage systems. The results obtained can be leveraged in the development of similar analyses in other countries where land subsidence due to deep mineral extraction is observed [15,59]. Nowadays, this is especially the case of coalfields in China, where coal mining is growing rapidly [10].

5. Conclusions

Surface subsidence due to deep underground extraction of minerals was revealed within a surface area of 38.8 km^2, which is 75.7% of the study area. At the end of the 19th century, absolute elevations ranged from 238 to 315 m a.s.l., and the elevation difference at that time was 77 m. At the end of the 20th century, absolute elevations ranged from 232 to 322 m a.s.l. After 111 years, the difference in elevations increased to 90 m. In some places, the maximum depressions reached a depth of almost 30 m.

By the end of the 19th century, the total length of the river network in the study area was 37.47 km. There were 192 anthropogenic reservoirs with a total surface area of 31.4 ha. The average reservoir surface area was less than 0.18 ha. By the end of the 20th century, the total length of the river network in the described area had decreased by 8.31 km, to 29.16 km. There were 322 anthropogenic water bodies functioning in the geographic environment during this period—an increase by 130 artificial lakes. Limnic waters covered a total surface area of 129.4 ha and the average reservoir surface area was 0.4 ha.

Changes in land reliefs have resulted in distinct water cycle disturbances at local and regional levels. Land subsidence disrupted the first-order watershed. Over a significant length it is uncertain, and in places—virtually impossible to delineate. Six basins have emerged that are isolated from their original catchments. In total, the endorheic areas spread over 6.9 km^2. Using average annual precipitation for 1961 to 2020—of 731.5 mm, it was calculated that just over 5 hm^3 of water enters the endorheic areas annually. The average annual field evaporation was 481.7 mm for this multi-year period, for a total average annual loss of 3.3 hm^3 of water. Consequently, this results in an average excess of 1.7 hm^3 of water per year in the water cycle in these areas.

Funding: This research was funded by University of Silesia in Katowice (Poland)—Institute of Earth Sciences, project no. WNP/INoZ/2020_ZB25.

Data Availability Statement: Data are contained within the article or supplementary material. Publicly available datasets were analyzed in this study. These data can be found here: Website of the Institute of Meteorology and Water Management—National Research Institute Available online: https://danepubliczne.imgw.pl/data/dane_pomiarowo_obserwacyjne/ (accessed on 11 May 2022).

Acknowledgments: I would like to thank the linguistic team for correcting the English language of the manuscript.

Conflicts of Interest: The author declare no competing interest.

References

1. Oki, T.; Kanae, S. Global hydrological cycles and world water resources. *Science* **2006**, *313*, 1068–1072. [CrossRef] [PubMed]
2. Bosilovich, M.G.; Schubert, S.D.; Walker, G.K. Global Changes of the Water Cycle Intensity. *J. Clim.* **2005**, *18*, 1591–1608. [CrossRef]
3. Levizzani, V.; Cattani, E. Satellite Remote Sensing of Precipitation and the Terrestrial Water Cycle in a Changing Climate. *Remote Sens.* **2019**, *11*, 2301. [CrossRef]
4. Drenkhan, F.; Carey, M.; Huggel, C.; Seidel, J.; Oré, M.T. The changing water cycle: Climatic and socioeconomic drivers of water-related changes in the Andes of Peru. *WIREs Water* **2015**, *2*, 715–733. [CrossRef]
5. Solarski, M.; Machowski, R.; Rzetala, M.; Rzetala, M.A. Hypsometric changes in urban areas resulting from multiple years of mining activity. *Sci. Rep.* **2022**, *12*, 2982. [CrossRef] [PubMed]
6. Ilie, O.; Dacian, M. Ground surface subsidence as effect of underground mining of the thick coal seams in the Jiu Valley Basin. *Arch. Min. Sci.* **2012**, *57*, 547–577. [CrossRef]
7. Abdikan, S.; Arikan, M.; Sanli, F.B.; Cakir, Z. Monitoring of coal mining subsidence in peri-urban area of Zonguldak city (NW Turkey) with persistent scatterer interferometry using ALOS-PALSAR. *Environ. Earth Sci.* **2014**, *71*, 4081–4089. [CrossRef]
8. Yuan, M.; Li, M.; Liu, H.; Lv, P.; Li, B.; Zheng, W. Subsidence Monitoring Base on SBAS-InSAR and Slope Stability Analysis Method for Damage Analysis in Mountainous Mining Subsidence Regions. *Remote Sens.* **2021**, *13*, 3107. [CrossRef]
9. Wang, Z.; Liu, Y.; Zhang, Y.; Liu, Y.; Wang, B.; Zhang, G. Spatially Varying Relationships between Land Subsidence and Urbanization: A Case Study in Wuhan, China. *Remote Sens.* **2022**, *14*, 291. [CrossRef]
10. Wang, J.; Lu, C.; Sun, Q.; Xiao, W.; Cao, G.; Li, H.; Yan, L.; Zhang, B. Simulating the hydrologic cycle in coal mining subsidence areas with a distributed hydrologic model. *Sci. Rep.* **2017**, *7*, 39983. [CrossRef]
11. Guzy, A.; Malinowska, A.A. Assessment of the Impact of the Spatial Extent of Land Subsidence and Aquifer System Drainage Induced by Underground Mining. *Sustainability* **2020**, *12*, 7871. [CrossRef]
12. Solarski, M. Anthropogenic transformations of the Bytom area relief in the period of 1883–1994. *Environ. Socio-Econ. Stud.* **2013**, *1*, 1–8. [CrossRef]
13. Machowski, R.; Rzetala, M.A.; Rzetala, M.; Solarski, M. Geomorphological and hydro-logical effects of subsidence and land use change in industrial and urban areas. *Land Degrad. Dev.* **2016**, *27*, 1740–1752. [CrossRef]
14. Szypuła, B. Quantitative changes of anthropogenic relief over the last 100 years in the Silesian Upland (south Poland). *Z. Geomorphol.* **2014**, *58*, 175–183. [CrossRef]
15. Marschalko, M.; Yilmaz, I.; Lamich, D.; Drusa, M.; Kubečková, M.; Peňaz, T.; Burkotová, T.; Slivka, V.; Bednárik, M.; Krčmář, D.; et al. Unique documentation, analysis of origin and development of an undrained depression in a subsidence basin caused by underground coal mining (Kozinec, Czech Republic). *Env. Earth Sci* **2014**, *72*, 11–20. [CrossRef]
16. Harnischmacher, S.; Zepp, H. Mining and its impact on the earth surface in the Ruhr District (Germany). *Z. Fur Geomorphol.* **2014**, *58* (Suppl. S3), 3–22. [CrossRef]
17. Zheng, L.; Zhu, L.; Wang, W.; Guo, L.; Chen, B. Land Subsidence Related to Coal Mining in China Revealed by L-Band InSAR Analysis. *Int. J. Environ. Res. Public Health* **2020**, *17*, 1170. [CrossRef]
18. Zheng, J.; Yao, W.; Lin, X.; Ma, B.; Bai, L. An Accurate Digital Subsidence Model for Deformation Detection of Coal Mining Areas Using a UAV-Based LiDAR. *Remote Sens.* **2022**, *14*, 421. [CrossRef]
19. Cabala, J.M.; Cmiel, S.R.; Idziak, A.F. Environmental impact of mining activity in the Upper Silesian Coal Basin (Poland). *Geol. Belg.* **2004**, *7*, 225–229.
20. Cheng, W.; Bian, Z.; Dong, J.; Lei, S. Soil properties in reclaimed farmland by filling subsidence basin due to underground coal mining with mineral wastes in China. *Trans. Nonferrous Met. Soc. China* **2014**, *24*, 2627–2635. [CrossRef]
21. Hürlimann, M.; Guo, Z.; Puig-Polo, C.; Medina, V. Impacts of future climate and land cover changes on landslide susceptibility: Regional scale modelling in the Val d' Aran region (Pyrenees, Spain). *Landslides* **2022**, *19*, 99–118. [CrossRef]
22. *Detailed Geological Map of Poland, 1:50,000*; Geological Publisher: Warsaw, Poland, 1954.
23. Jones, A.; Duck, R.; Reed, R.; Weyers, J. *Practical Skills in Environmental Science*; Prentice Hall: London, UK, 2000.
24. *Topographic map (Topographische karte), 1:25,000.*; Messtischblatt, 5679-Beuthen: Berlin, Germany, 1934.
25. *Topographic map (Topographische karte), 1:25,000.*; Messtischblatt, 5779-Schwientochlowitz: Berlin, Germany, 1929.
26. *Topographic map of Poland, 1: 10,000; M-34-62-B-a-2 (Ruda Śląska-Ruda), M-34-62-B-a-4 (Ruda Śląska), M-34-62-B-b-1 (Świętochłowice), M-34-62-B-b-3 (Ruda Śląska-Kochłowice)*; Chief Land Surveyor: Warsaw, Poland, 1994.
27. Gutry-Korycka, M.; Werner-Więckowska, H. *Guide to Hydrographic Field Research*; Polish Scientific Publishers: Warsaw, Poland, 1989.
28. Machowski, R.; Rzetala, M. Impact of subsidence basins on changes in the catchment water cycle. In *International Multidiscyplinary Scientific Geoconferences, Proceedings of the 18th GeoConference on Water Resources. Forest, Marine and Ocean Ecosystems, Albena, Bulgaria, 30 June–9 July 2018*; Albena, Bulgaria, 30 June–9 July 2018, STEF92 Technology Ltd.: Sofia, Bulgaria, 2018; pp. 407–414. [CrossRef]
29. Liu, S.; Han, Y.; Su, H. Regional Evapotranspiration Estimation by the Improved MOD16-sm Model and Its Application in Central China. *Water* **2022**, *14*, 1491. [CrossRef]
30. Jiao, P.; Hu, S.-J. Optimal Alternative for Quantifying Reference Evapotranspiration in Northern Xinjiang. *Water* **2022**, *14*, 1. [CrossRef]

31. Althoff, D.; Santos, R.A.d.; Bazame, H.C.; Cunha, F.F.d.; Filgueiras, R. Improvement of Hargreaves–Samani Reference Evapotranspiration Estimates with Local Calibration. *Water* **2019**, *11*, 2272. [CrossRef]
32. Valipour, M. Temperature analysis of reference evapotranspiration models. *Meteorol. Appl.* **2015**, *22*, 385–394. [CrossRef]
33. Hargreaves, G.L.; Samani, Z.A. Evapotranspiration from temperature. *Appl. Eng. Agric.* **1985**, *1*, 96–99. [CrossRef]
34. McKenney, M.S.; Rosenberg, N.J. Sensitivity of some potential evapotranspiration estimation methods to climate change. *Agric. For. Meteorol.* **1993**, *64*, 81–110. [CrossRef]
35. Dynowska, I.; Dynowski, J. *Hydrographical Exercises for Geographers*; Jagiellonian University: Cracow, Poland, 1982.
36. Różkowski, J.; Pacholewski, A. Water balances of representative catchments in the carbonate Jura formations of the Kraków-Wieluń Upland (Polish). *Przegląd Geol.* **1996**, *44*, 850–854.
37. Available online: https://www.gov.pl/attachment/8530a475-f8dc-4ae0-af57-1ff5b7da7342 (accessed on 26 August 2022).
38. Choiński, A. *Physical Limnology of Poland*; Adam Mickiewicz University: Poznań, Poland, 2007.
39. *Hydrographic map of Poland, 1:50 000. Sheet: M-34-62-B (Chorzów)*; Chief Land Surveyor: Warsaw, Poland, 2001.
40. Sopata, P.; Stoch, T.; Wójcik, A.; Mrocheń, D. Land Surface Subsidence Due to Mining-Induced Tremors in the Upper Silesian Coal Basin (Poland)–Case Study. *Remote Sens.* **2020**, *12*, 3923. [CrossRef]
41. Abramowicz, A.; Rahmonov, O.; Chybiorz, R. Environmental Management and Landscape Transformation on Self-Heating Coal-Waste Dumps in the Upper Silesian Coal Basin. *Land* **2021**, *10*, 23. [CrossRef]
42. Dulias, R. *The Impact of Mining on the Landscape, A Study of the Upper Silesian Coal Basin in Poland*; Environmental Science and Engineering; Springer International Publishing: Cham, Switzerland, 2016.
43. Rahmonov, O.; Krzysztofik, R.; Środek, D.; Smolarek-Lach, J. Vegetation- and Environmental Changes on Non-Reclaimed Spoil Heaps in Southern Poland. *Biology* **2020**, *9*, 164. [CrossRef] [PubMed]
44. Woźniak, G.; Dyderski, M.K.; Kąpała-Bomba, A.; Jagodziński, A.M.; Pasierbiński, A.; Błońska, A.; Bierza, W.; Magurno, F.; Sierka, E. Use of Remote Sensing to track post-industrial vegetation development. *Land Degrad. Dev.* **2021**, *32*, 1426–1439. [CrossRef]
45. Dwucet, K.; Wach, J. Calculation of land surface changes caused by deep mining exploitation on the example of Katowice voivodeship. In *A guide to Exercises in Environmental Protection*; University of Economics: Katowice, Poland, 1994; pp. 95–97.
46. Luo, M.; Liu, Y.; Shao, T. Response of Drylands' Water-cycle to the Global Warming. *Int. J. Climatol.* **2021**, *41*, 4587–4602. [CrossRef]
47. Yoon, J.H.; Wang, S.Y.; Gillies, R.; Kravitz, B.; Hipps, L.; Rash, P.J. Increasing water cycle extremes in California and in relation to ENSO cycle under global warming. *Nat. Commun.* **2015**, *6*, 8657. [CrossRef] [PubMed]
48. Xu, Z.; Cheng, L.; Luo, P.; Liu, P.; Zhang, L.; Li, F.; Liu, L.; Wang, J. A Climatic Perspective on the Impacts of Global Warming on Water Cycle of Cold Mountainous Catchments in the Tibetan Plateau: A Case Study in Yarlung Zangbo River Basin. *Water* **2020**, *12*, 2338. [CrossRef]
49. Coe, M.T.; Foley, J.A. Human and natural impacts on the water resources of the Lake Chad basin. *J. Geophys. Res.-Atmos.* **2001**, *106*, 3349–3356. [CrossRef]
50. Hu, Z.; Chen, X.; Zhou, Q.; Yin, G.; Liu, J. Dynamical variations of the terrestrial water cycle components and the influences of the climate factors over the Aral Sea Basin through multiple datasets. *J. Hydrol.* **2022**, *604*, 127270. [CrossRef]
51. Allies, A.; Demarty, J.; Olioso, A.; Bouzou Moussa, I.; Issoufou, H.B.-A.; Velluet, C.; Bahir, M.; Maïnassara, I.; Oï, M.; Chazarin, J.-P.; et al. Evapotranspiration Estimation in the Sahel Using a New Ensemble-Contextual Method. *Remote Sens.* **2020**, *12*, 380. [CrossRef]
52. Rösler, A. Comparasion of evaporation conditions from a sunken and floating pans on Lake Sława. *Limnol. Rev.* **2002**, *2*, 333–341.
53. Xu, C.-Y.; Singh, V.P. Evaluation of three complementary relationship evapotranspiration models by water balance approach to estimate actual regional evapotranspiration in different climatic regions. *J. Hydrol.* **2005**, *308*, 105–121. [CrossRef]
54. Al-Ghobari, H.M. Estimation of reference evapotranspiration for southern region of Saudi Arabia. *Irrig. Sci.* **2000**, *19*, 81–86. [CrossRef]
55. Tandogdu, Y.; Camgoz, O. An experimental approach for estimating evapotranspiration. *Cim Bulletin* **1999**, *92*, 55–60.
56. Dulias, R. Impact of mining subsidence on the relief of the Rybnik Plateau, Poland. *Z. Für Geomorphol.* **2011**, *55*, 25–36. [CrossRef]
57. Bell, F.; Stacey, T.; Genske, D. Mining subsidence and its effect on the environment: Some differing examples. *Environ. Geol.* **2000**, *40*, 135–152. [CrossRef]
58. Rurek, M.; Gonia, A.; Hojan, M. Environmental and Socio-Economic Effects of Underground Brown Coal Mining in Piła Młyn (Poland). *Land* **2022**, *11*, 219. [CrossRef]
59. Harnischmacher, S. Quantification of mining subsidence in the Ruhr District (Germany). *Géomorphologie Relief Process. Environ.* **2010**, *16*, 261–274. [CrossRef]
60. Wright, P.; Stow, R. Detecting mining subsidence from space. *Int. J. Remote Sens.* **1999**, *20*, 1183–1188. [CrossRef]
61. Fan, H.; Gao, X.; Yang, J.; Deng, K.; Yu, Y. Monitoring Mining Subsidence Using A Combination of Phase-Stacking and Offset-Tracking Methods. *Remote Sens.* **2015**, *7*, 9166–9183. [CrossRef]
62. Fan, H.; Wang, L.; Wen, B.; Du, S. A New Model for three-dimensional Deformation Extraction with Single-track InSAR Based on Mining Subsidence Characteristics. *Int. J. Appl. Earth Obs. Geoinf.* **2021**, *94*, 102223. [CrossRef]
63. Zhang, B.; Lu, C.; Wang, J.; Sun, Q.; He, X.; Cao, G.; Zhao, Y.; Yan, L.; Gong, B. Using storage of coal-mining subsidence area for minimizing flood. *J. Hydrol.* **2019**, *572*, 571–581. [CrossRef]
64. Rzetala, M.; Jagus, A. New lake district in Europe: Origin and hydrochemical characteristics. *Water Environ. J.* **2011**, *26*, 108–117. [CrossRef]

65. Quanyuan, W.; Jiewu, P.; Shanzhong, Q.; Yiping, L.; Congcong, H.; Tingxiang, L.; Limei, H. Impacts of coal mining subsidence on the surface landscape in Longkou city, Shandong Province of China. *Environ. Earth Sci.* **2009**, *59*, 783–791. [CrossRef]
66. Fan, T.; Yan, J.; Wang, S.; Zhang, B.; Ruan, S.; Zhang, M.; Li, S.; Chen, Y.; Liu, J. Water quality variation of mining-subsidence lake during the initial stage: Cases study of Zhangji and Guqiao Mines. *J. Coal Sci. Eng.* **2012**, *18*, 297–301. [CrossRef]
67. Zhang, M.; Yuan, X.; Guan, D.; Liu, H.; Zhang, G.; Wang, K.; Zhou, L.; Wu, S.; Sun, K. Eco-exergy Evaluation of New Wetlands in the Yanzhou Coalfield Subsidence Areas Using Structural-Dynamic Modelling. *Mine Water Env.* **2019**, *38*, 746–756. [CrossRef]
68. Pierzchała, Ł.; Sierka, E. Do submerged plants improve the water quality in mining subsidence reservoirs? *Appl. Ecol. Environ. Res.* **2020**, *18*, 5661–5672. [CrossRef]